

Quantitative Measurements of Edge-to-Face Aromatic Interactions by Using Chemical Double-Mutant Cycles

Fiona J. Carver,^[a] Christopher A. Hunter,*^[a] Philip S. Jones,^[b] David J. Livingstone,^[c] James F. McCabe,^[a] Eileen M. Seward,^[d] Pascale Tiger,^[a] and Sharon E. Spey^[a]

Abstract: Synthetic H-bonded zipper complexes have been used to quantify the magnitude of an edge-to-face aromatic interaction between a benzoyl group and an aniline ring. Four chemical double-mutant cycles were constructed by using a matrix of nine closely related complexes in which the aromatic rings were sequentially substituted for alkyl

substituents. The stability constants and three-dimensional structures of the complexes were determined by using

Keywords: double-mutant cycle • edge-to-face interaction • hydrogen bonds • molecular recognition • pi interactions

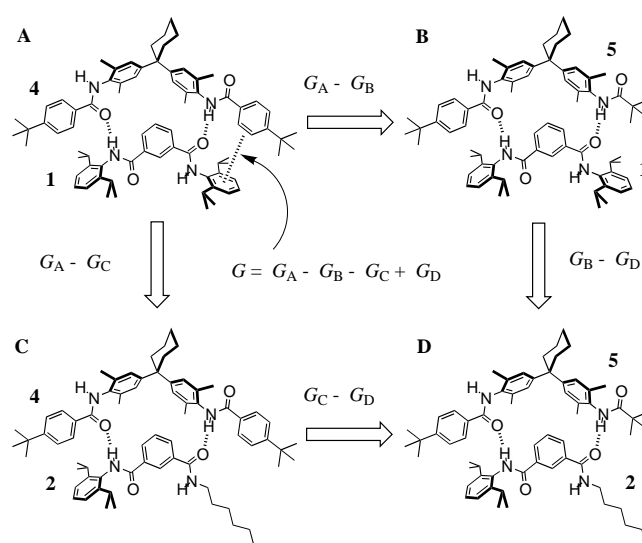
¹H NMR titrations in deuteriochloroform at room temperature. The value of the interaction energy is similar in all cases, the average is -1.4 ± 0.5 kJ mol⁻¹. The scope and limitations of the double-mutant approach are explored, and the consequences of conformational equilibria are discussed.

Introduction

Molecular recognition events generally involve the cooperation of a large number of weak noncovalent interactions to produce a significant thermodynamic driving force for binding. At present, the study of these events is at a qualitative rather than quantitative level: it is impossible to predict a binding constant (or binding enthalpy) even for a very simple system where the individual noncovalent interactions are straightforward to identify, let alone for a complicated biological macromolecule.^[1] The development of a more quantitative understanding of molecular recognition requires accurate measurements of noncovalent interaction energies and associated structure–activity relationships, but this is difficult to achieve, because the systems that must be studied to obtain this information are necessarily complex.^[2] One

approach is the study of synthetic supramolecular systems, which are relatively simple: they contain a small number of noncovalent interaction sites, but enough to cause complexation; they have limited conformational flexibility; structural modifications can be achieved readily through synthesis; characterisation is straightforward with conventional techniques.^[3]

We have selected the H-bonded “zipper” complex shown in Scheme 1 (Complex A, **1·4**) as a suitable system for making quantitative measurements of noncovalent functional-group



Scheme 1. A chemical double-mutant cycle for determining the magnitude of the terminal aromatic interaction in Complex A (**1·4**).

[a] Prof. C. A. Hunter, F. J. Carver, J. F. McCabe, P. Tiger, S. E. Spey
Centre for Chemical Biology
Krebs Institute for Biomolecular Science
Department of Chemistry, University of Sheffield
Sheffield, S3 7HF (UK)
Fax: (+44) 114-273-8673
E-mail: c.hunter@sheffield.ac.uk

[b] Dr. P. S. Jones
Roche Discovery Welwyn, 40 Broadwater Road
Welwyn Garden City, Herts, AL7 3AY (UK)

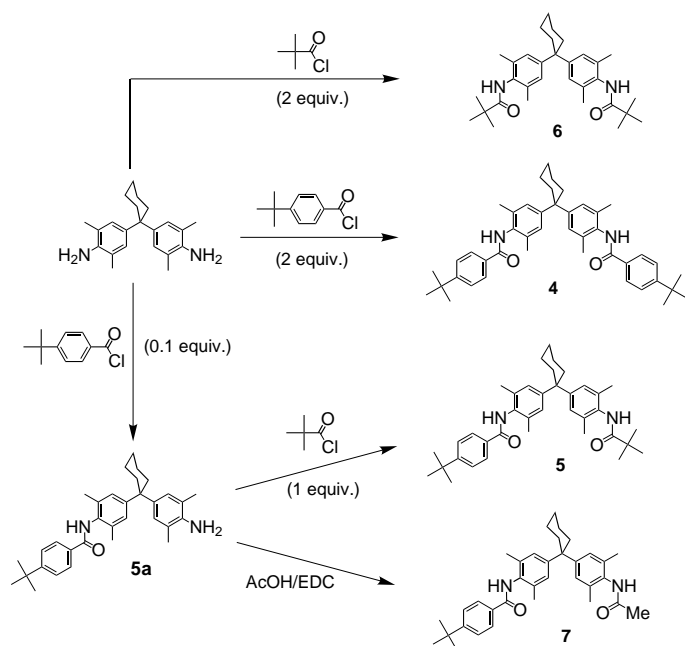
[c] Dr. D. J. Livingstone
ChemQuest, Delamere House, 1 Royal Crescent
Sandown, Isle of Wight, PO36 8LZ (UK)

[d] Dr. E. M. Seward
Merck Sharp and Dohme Research Laboratories
Neuroscience Research Centre, Terlings Park
Eastwick Road, Harlow, Essex, CM20 2QR (UK)

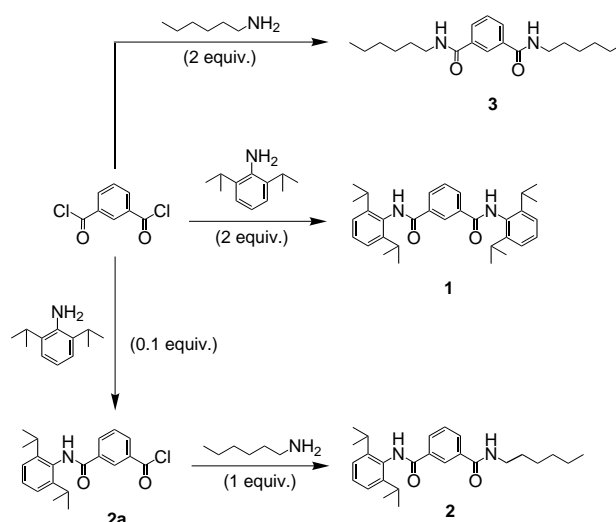
interaction energies.^[4] The complex is held together by two H-bonds and four aromatic interactions, and the stability constant is 48 M^{-1} in chloroform; this means the free energy of binding can readily be determined by NMR titrations. The component molecules have no free rotors (although there are some conformational equilibria, which will be discussed later), and so the loss of conformational entropy on binding is small. The three-dimensional solution structure of the complex can be determined by using intermolecular NOEs and the complexation-induced changes in chemical shift,^[5] and all of this information can be collected easily. The approach we have taken to quantifying specific functional-group contributions to the overall binding energy of this system is the double-mutant method, which has been widely used in protein engineering experiments to quantify amino acid side-chain interactions.^[2a–c] The principles are explained below, but essentially we are removing the interaction of interest by a chemical mutation and quantifying how that affects the stability of the complex. The zipper complex is ideally suited to this approach, because we can make changes to the terminal functional groups without affecting the core of the complex. There are problems associated with the macrocyclic and cleft architectures more commonly used in host–guest chemistry, since it is difficult to make such mutations without having a more drastic effect on the structure.

Results and Discussion

The compounds required to construct chemical double-mutant cycles based on the zipper complex (**1**·**4**) were prepared according to Schemes 2 and 3 by using simple amide coupling reactions. A carbodiimide coupling reagent (1-(3-dimethylaminopropyl)-3-ethylcarbodiimide—EDC) was used to acetylate **5a**, because the use of acetyl chloride led to



Scheme 2. Synthesis of compounds **4**–**7**.



Scheme 3. Synthesis of compounds **1**–**3**.

contamination with the imide. All other steps were straightforward and proceeded in good yield.

Scheme 1 illustrates the first double-mutant cycle we examined and will be used to explain the approach. In principle, the magnitude of the terminal aromatic interaction highlighted in Complex A (**1**·**4**) in Scheme 1 can be estimated by chemical mutations which remove it, that is by comparing the stability of Complex A with complexes B or C, which do not have this interaction present. However, this assumes that the aromatic rings in question make no other intermolecular interactions in Complex A and that the strength of the H-bonds remains constant when the aromatic to alkyl mutation is made. These effects can be quantified by using the double-mutant, Complex D. For example, if we compare complexes C and D, the difference $\Delta G_C - \Delta G_D$ is a direct measure of the sum of the change in H-bond strength and secondary interactions made by the benzoyl group in complexes A and C. Thus the free energy difference of the two horizontal (or vertical) mutations in Scheme 1 allows us to dissect the interaction of interest from the complicated array of weak interactions present in Complex A.

Equation (1), aromatic interaction in Complex A:

$$\Delta\Delta G = \Delta G_A - \Delta G_B - \Delta G_C + \Delta G_D \quad (1)$$

There are a number of assumptions inherent in this analysis, which we will discuss presently. However, we emphasise that this is a practical experimental approach that solves a lot of the problems generally associated with the quantification of weak intermolecular forces in complicated systems. The most important assumption is that the functional groups used in the mutations, the hexyl and *tert*-butyl groups, do not interact with the adjacent aromatic rings (evidence for this assertion will be presented later). Secondly, we assume that the sum of free energy changes measured here corresponds to a functional group interaction enthalpy; in other words that the entropy changes cancel out in the cycle and that entropy–enthalpy compensation is not a significant factor in this system.^[6] We also assume that the secondary interactions and changes in

H-bond strength are additive functions of the mutations. Theoretically, the energy of a H-bond is proportional to the product of the dipole moments.^[7] However, in the limit of a small change in dipole moment, the change in the product is approximately equal to the change in the sum. For example, if the amide dipole moments in Complex A, μ_1 and μ_2 , change by small amounts, $\delta\mu_1$ and $\delta\mu_2$, when they are mutated, the H-bond strengths in the four complexes in the double-mutant cycle are given by Equations (2)–(5):

$$\text{H-bond in Complex A} = c\mu_1\mu_2 \quad (2)$$

$$\begin{aligned} \text{H-bond in Complex B} &= c\mu_1(\mu_2 + \delta\mu_2) \\ &= c\mu_1\mu_2 + c\mu_1\delta\mu_2 \end{aligned} \quad (3)$$

$$\begin{aligned} \text{H-bond in Complex C} &= c(\mu_1 + \delta\mu_1)\mu_2 \\ &= c\mu_1\mu_2 + c\mu_2\delta\mu_1 \end{aligned} \quad (4)$$

$$\begin{aligned} \text{H-bond in Complex D} &= c(\mu_1 + \delta\mu_1)(\mu_2 + \delta\mu_2) \\ &= c\mu_1\mu_2 + c\mu_1\delta\mu_2 + c\mu_2\delta\mu_1 + c\delta\mu_1\delta\mu_2 \end{aligned} \quad (5)$$

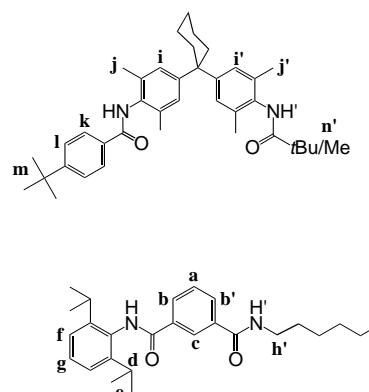
Putting these values into the double-mutant cycle Equation (1), the residual contribution due to changes in H-bond strength is given by Equation (6)

$$\Delta(\text{H-bond}) \approx c\delta\mu_1\delta\mu_2 \quad (6)$$

If the changes $\delta\mu_1$ and $\delta\mu_2$ are small relative to μ_1 and μ_2 , then this will be a very small energy. In other words, for small changes in the polarity of the amide groups, the double-mutant cycle is valid. As we will see, the change in H-bond strength and secondary interactions in this system are rather small, and so the approach is not compromised by the nonadditivity of the H-bond energies.

Clearly to use this approach in practice, two things are required: an accurate evaluation of the stability constants of all four complexes in a cycle and evidence that the three-dimensional structure of the core of the complex is unaffected by the peripheral mutations. ¹H NMR titrations and NOE experiments provide this information. The data for all of the complexes studied are listed in Table 1. We will begin by

considering the double-mutant cycle in Scheme 1. All of the complexes show intermolecular NOEs between the bisaniline methyl groups, **j** and **j'**, and the isophthaloyl protons, **a** and **b** (Scheme 4). Where terminal aromatic groups are present,



Scheme 4. Proton labelling scheme for the complexes.

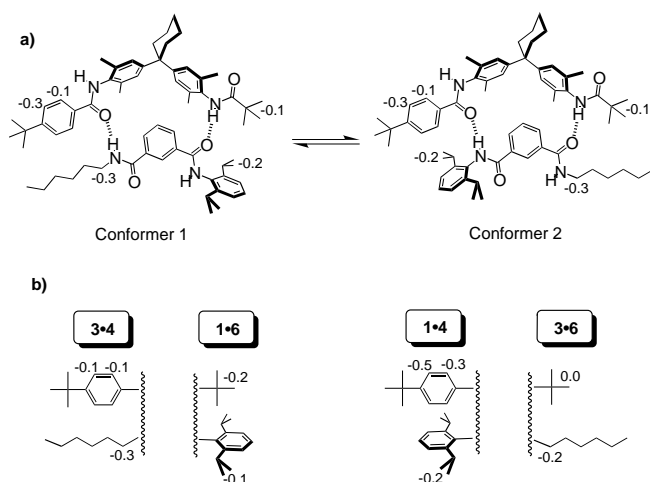
intermolecular NOEs are observed between the isopropyl methyl groups, **e**, and the benzoyl protons, **l** and **k**. These NOEs locate the isophthaloyl group in the bisaniline pocket and the benzoyl and aniline groups in close proximity, as shown in Scheme 1. The limiting complexation-induced changes in chemical shift ($\Delta\delta$ values) for the central isophthaloyl, **NH**, **NH'**, **a**, **b**, **b'**, **c**, and bisaniline, **NH**, **NH'**, **i**, **i'**, **j**, **j'**, protons are almost identical for all four complexes (Table 1, Complex A = **1·4**, B = **1·5**, C = **2·4**, D = **2·5**); this shows that the structure of the core of the complex is unaffected by the mutations. However, if we examine the peripheral mutated functional groups, it becomes clear that there is a problem with this system. Complex D can exist as two different conformational isomers (Figure 2), and the $\Delta\delta$ values suggest that both are present in similar proportions. The expected $\Delta\delta$ values if only Conformer 2 were present can be estimated from complexes **1·4** and **3·6**, where this conformational ambiguity does not exist and where the

Table 1. ¹H NMR titration data (in deuteriochloroform at 295 K).^[a]

Complex	K_a M ⁻¹	ΔG kJ mol ⁻¹	Limiting Complexation-induced changes in ¹ H NMR chemical shift. ^[b]																				
			Isophthaloyl component										Bisaniline component										
			NH	NH'	a	b	b'	c	d	e	f	g	h'	NH	NH'	i	i'	j	j'	k	l	m	n'
1·4	48 ± 2	-9.5 ± 0.1	+1.4	-	-1.6	-0.4	-	0.0	0.0	-0.2	0.0	+0.1	-	+1.1	-	+0.2	-	0.0	-	-0.3	-0.5	-0.1	-
1·5	17 ± 1	-6.9 ± 0.1	+1.4	-	-1.7	-0.6	-	0.0	-0.1	-0.2	-0.1	0.0	-	+0.9	+0.6	+0.2	+0.2	-0.1	0.0	-0.2	-0.4	0.0	-0.2
1·6	12 ± 1	-6.0 ± 0.2	+1.1	-	-1.5	-0.4	-	0.0	0.0	0.0	0.0	0.0	-	-	+0.9	-	+0.1	-	0.0	-	-	-	-0.2
2·4	20 ± 2	-7.3 ± 0.3	+1.4	+1.0	-1.5	-0.2	-0.5	0.0	0.0	-0.1	0.0	0.0	-0.1	+0.9	-	+0.1	-	-0.1	-	-0.1	-0.2	0.0	-
2·5	10 ± 1	-5.6 ± 0.3	+1.6	+1.0	-1.5	-0.3	-0.7	0.0	0.0	-0.2	-0.1	0.0	-0.3	+1.3	+0.6	+0.1	+0.1	-0.1	0.0	-0.1	-0.3	-0.1	-0.1
2·6	8 ± 1	-5.2 ± 0.3	+0.9	+0.8	-1.1	-0.2	-0.6	0.0	0.0	0.0	0.0	0.0	-0.2	-	-	+0.6	-	0.0	-	-0.1	-	-	-0.2
3·4	15 ± 1	-6.6 ± 0.2	-	+1.1	-0.8	-	-0.3	0.0	-	-	-	-	-0.3	+0.9	-	0.0	-	-0.1	-	-0.1	-0.1	0.0	-
3·5	10 ± 1	-5.6 ± 0.3	-	+1.0	-0.8	-	-0.4	0.0	-	-	-	-	-0.3	+1.3	+1.1	0.0	0.0	-0.2	-0.1	-0.1	-0.1	0.0	0.0
3·6	10 ± 1	-5.6 ± 0.3	-	+0.7	-0.7	-	-0.4	0.0	-	-	-	-	-0.2	-	+0.6	-	0.0	-	-0.1	-	-	-	0.0
1·7	15 ± 1	-6.7 ± 0.1	+1.6	-	-1.5	-0.4	-	0.0	-0.1	-0.2	0.0	0.0	-	nd ^[c]	nd	nd	nd	nd	nd	nd	nd	nd	nd
2·7	9 ± 1	-5.4 ± 0.2	-	+1.4	-1.8	-0.4	-0.4	0.0	-0.1	-0.2	0.0	0.0	-0.3	nd	nd	nd	nd	nd	nd	nd	nd	nd	nd
3·7	8 ± 2	-5.2 ± 0.5	-	+0.8	-0.7	-	-0.4	0.0	-	-	-	-	-0.3	nd	nd	nd	nd	nd	nd	nd	nd	nd	nd

[a] Average values from at least three separate experiments. Titration data for 4–6 different signals were used to determine the association constant in each experiment. Errors are quoted as twice the standard error from the weighted mean (weighting based on the observed change in chemical shift). [b] Calculated by extrapolating titration data for formation of 1:1 complexes in deuteriochloroform at 295 K (see Scheme 4 for proton labelling scheme). Dashes indicate signals that do not exist in the complex concerned. [c] Not determined.

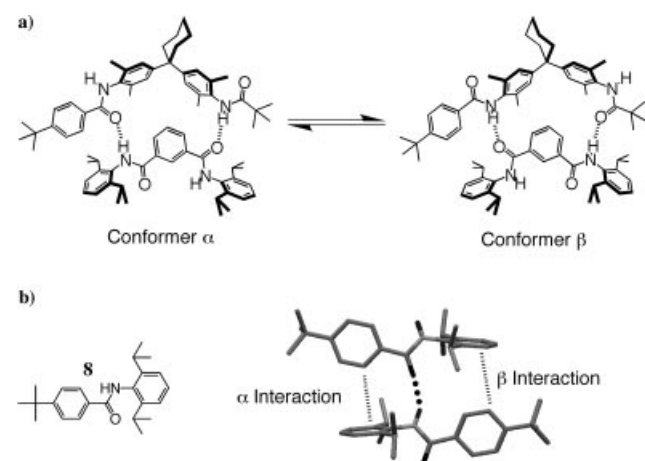
relative positions of the terminal functional groups are identical (Scheme 5, Table 1). Similarly, expected $\Delta\delta$ values for Conformer 1 can be estimated from complexes **1**•**6** and **3**•**4**. The observed $\Delta\delta$ values for **2**•**5**, particularly for signal **1**, which shows the largest changes, look like a 1:1 mixture of the



Scheme 5. Conformational equilibrium in the **2**•**5** complex. Conformer 1 contains one benzoyl–hexyl interaction and one *tert*-butyl–aniline interaction, and so should show the same $\Delta\delta$ values as complexes **3**•**4** and **1**•**6**. Conformer 2 contains one benzoyl–aniline interaction and one *tert*-butyl–hexyl interaction, and so should show the same $\Delta\delta$ values as complexes **1**•**4** and **3**•**6**. The $\Delta\delta$ values for these four complexes are illustrated, and the experimental values for the **2**•**5** complex are shown.

two conformers. This clearly invalidates the double-mutant cycle in Scheme 1, since there is a change in the structure of the core of the complex in Conformer 1 of Complex D.

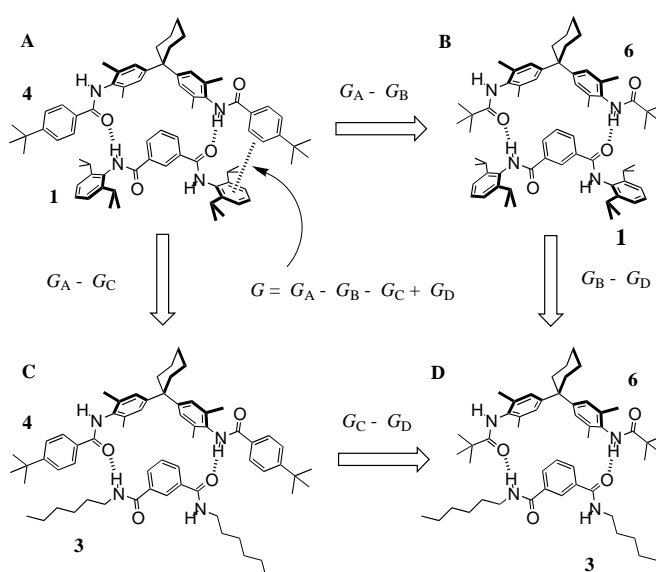
If we consider the structures of the complexes in more detail, there are other conformational equilibria present. For example, Complex B can exist in two forms (Scheme 6a) that



Scheme 6. Conformational equilibrium in the **1**•**5** complex. The difference between conformers α and β is the orientation of the amide groups and H-bonds. This leads to a subtle difference in the orientation of the interaction between the terminal functional groups. The crystal structure of compound **8**, shown at the bottom, illustrates this difference: the edge-to-face interaction labelled α involves the amide oxygen as the H-bond acceptor and close contact between the benzoyl α proton and the face of the aniline ring, while the interaction labelled β involves the amide NH as the H-bond donor and close contact between the benzoyl β proton and the face of the aniline ring.

differ in the orientation of the H-bonds. The X-ray crystal structure of the model compound **8** suggests that this difference has a subtle effect on the relative geometries of the interacting groups (Scheme 6b): for Conformer α , it is the α proton of the benzoyl group that is closest to the aniline ring, whereas in Conformer β , it is the β proton that is closest to the aniline ring. These conformational equilibria are present in all complexes that involve nonsymmetrical components. However, the only real difference is a slight rotation of the terminal functional groups, and for the purposes of this study, we assume that such a subtle change has a negligible effect on the aromatic interaction. In fact, what the double-mutant cycle measures is a Boltzmann weighted average of the interaction energies for the two different geometries.

We can construct a double-mutant cycle that avoids all of these conformational problems by using symmetric compounds to measure the sum of the two terminal aromatic interactions (Scheme 7). For this system, although the pattern



Scheme 7. A chemical double-mutant cycle for determining the magnitude of both terminal aromatic interactions in Complex A (**1**•**4**). The complexes in this cycle contain only symmetrical compounds, and so the problems of conformational equilibria are avoided.

of $\Delta\delta$ values in the core of the complex is maintained on mutation, the magnitudes of the changes differ significantly. The $\Delta\delta$ values for the isophthaloyl proton **a** in complexes involving **3** are low ($\delta = -0.8$) relative to the complexes involving **1** ($\delta = -1.6$). This suggests a subtle change in structure associated with the aniline to hexyl mutation. However, the double-mutant cycle is specifically designed to factor out such effects, because two of the complexes involve the hexyl derivative **3** and two involve the aniline derivative **1**. For example, the change in the free energy of the core of the complex associated with the vertical aniline to hexyl mutation in Scheme 7 appears in the term $\Delta G_A - \Delta G_C$ as well as in the term $\Delta G_B - \Delta G_D$. The difference in these two terms is what we use to obtain the functional group interaction energy, $\Delta\Delta G$, and so the thermodynamic effects of the subtle differences in conformation cancel out.

In order to check that the variation in the $\Delta\delta$ values really does represent a subtle conformational change rather than some dramatic rearrangement of the structure that would invalidate the double-mutant cycle, we used the chemical-shift data and NOEs to determine the three-dimensional solution structure of Complex **3**•**4**, which shows the largest deviations from the values observed for Complex **1**•**4**.^[5] The NMR structures of the **3**•**4** and **1**•**4** complexes are compared in Figure 1. The structures are very similar, with two H-bonds and the isophthaloyl group docked into the centre of the bisaniline pocket. Figure 1b highlights the major difference between the two structures that causes the variation in the $\Delta\delta$ values for the isophthaloyl protons. In the **1**•**4** complex, the 2,6-diisopropyl anilines form a groove into which the benzoyl groups fit snugly. Removing this steric restriction appears to give the **3**•**4** complex more flexibility, so that the isophthaloyl group can tilt out of the bisaniline pocket while maintaining the two H-bond interactions. The NMR structure-determination method produces a single structure that best matches the experimental $\Delta\delta$ values, but in reality the observed $\Delta\delta$ values are a weighted average of all conformations present. The tilting of the isophthaloyl group in the bisaniline pocket is most likely a dynamic process, and the tilted structure in Figure 1b represents a time-averaged displacement from the symmetric, flat conformation.

Thus the structures of the complexes in Scheme 7 are suitable for the double-mutant cycle approach. By using the free energies of complexation in Table 1, the sum of the two terminal aromatic interactions is evaluated as $2.5 \pm 0.6 \text{ kJ mol}^{-1}$ in chloroform. The potential energy surface for aromatic interactions of this type is rather flat, and so it is unlikely that the α and β interactions in Scheme 6 differ significantly. If we assume that there is no difference, the magnitude of one edge-to-face aromatic interaction in this system is $-1.3 \pm 0.3 \text{ kJ mol}^{-1}$. This is a weak interaction, but as we have shown, it is very sensitive to substituent effects.^[4c, 8]

If we consider all possible complexes that can be formed from compounds **1**–**6**, we can construct a 3×3 grid of mutant complexes based on **1**•**4** (Figure 2). As long as we avoid the central **2**•**5** complex that suffers from the conformational problems illustrated in Scheme 5, it is possible to construct a range of four component double-mutant cycles from this grid. The $\Delta\delta$ values in Table 1 show that the structures of the cores of the complexes are essentially identical in all nine systems as discussed above. The 3×3 grid in Figure 2 produces two new double-mutant cycles that give the magnitude of one edge-to-face

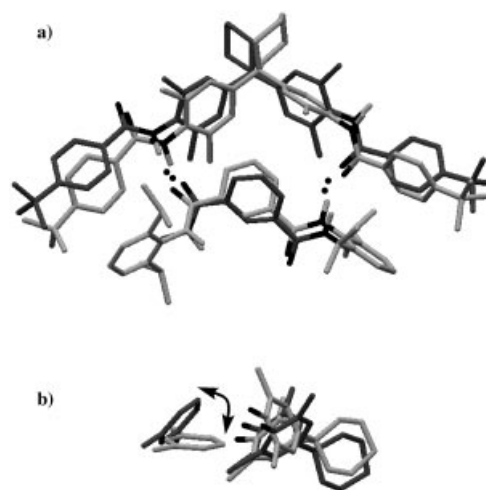


Figure 1. The NMR solution structures of complexes **1**•**4** (pale) and **3**•**4** (dark). These structures were calculated by using the experimental $\Delta\delta$ values in Table 1 and intermolecular NOEs from ROESY experiments. a) An overlay of the two structures. Only the first CH_2 group of the hexyl chain was used in the calculation, because the changes in chemical shift for the other chain protons were small. The hexyl group is, in any case, conformationally flexible and unlikely to adopt an ordered structure. The conformation of the cyclohexyl group is not defined by the calculation, since there are no complexation-induced changes in chemical shift for these protons. b) An orthogonal view of the complex showing only the isophthaloyl and bisaniline groups. This highlights the major difference between the two structures: the tilting of the isophthaloyl group out of the bisaniline pocket in the **3**•**4** complex.

interaction as $-1.6 \pm 0.4 \text{ kJ mol}^{-1}$ and $-1.4 \pm 0.5 \text{ kJ mol}^{-1}$ as indicated. These new cycles both involve the use of a nonsymmetric compound, and so there is an ambiguity caused by the α – β conformational equilibrium (Scheme 6). The measurements therefore represent a Boltzmann average of

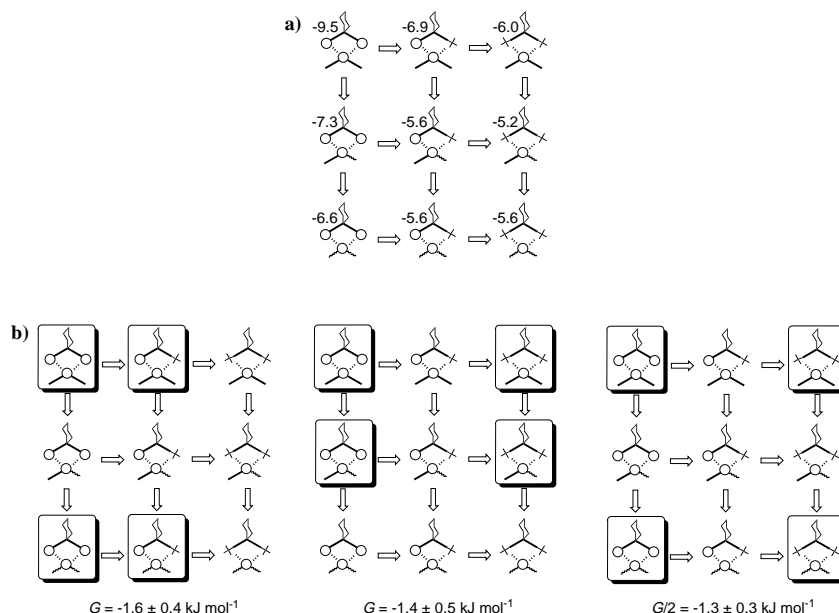


Figure 2. a) Schematic representation of the 3×3 grid of all possible complexes which can be formed from compounds **1**–**6**. The free energies of complexation in kJ mol^{-1} are indicated. b) The boxes highlight three double-mutant cycles that can be extracted from this grid avoiding the central **2**•**5** complex, which is conformationally unstable. The magnitude of the benzoyl–aniline edge-to-face aromatic interaction determined by using each cycle is shown.

the interactions in these two conformations in the relevant complexes. However, the final values for the aromatic interaction energy agree well with the interaction measured in the symmetric cycle; this suggests that this is not a serious problem, that is the conformational equilibrium in Scheme 6 does not have a significant effect on the aromatic interaction energy.

We now return to the double-mutant cycle in Scheme 1, and the problems encountered with the conformational equilibria in Complex D (the **2**·**5** complex). If we take a closer look at Scheme 5, it is clear that the interactions involved on the two sides of the conformational equilibrium are identical to the interactions the double-mutant cycle is used to quantify. Conformer 2 features the aromatic interaction of interest found in Complex A as well as the interactions found in the double-mutant, Complex D, whereas Conformer 1 contains the two interactions found in the single mutants, Complexes B and C. Thus the four complexes used to predict the $\Delta\delta$ values for the **2**·**5** complex might also be useful for predicting the free energy difference between Conformers 1 and 2 [Eq. (7)].

$$2(\Delta G_2 - \Delta G_1) \approx \{\Delta G(\mathbf{1} \cdot \mathbf{4}) + \Delta G(\mathbf{3} \cdot \mathbf{6})\} - \{\Delta G(\mathbf{3} \cdot \mathbf{4}) + \Delta G(\mathbf{1} \cdot \mathbf{6})\} \quad (7)$$

However, the sum in Equation (7) is identical to the sum used in Scheme 7 to evaluate the aromatic interaction in the symmetric double-mutant cycle. Thus the free energy difference between Conformer 1 and Conformer 2 corresponds to the $\Delta\Delta G$ for one aromatic interaction evaluated in a double-mutant cycle. It is therefore possible to draw up a set of simultaneous equations that can be used to obtain another independent measure of the aromatic interaction in this system by using the double-mutant cycle shown in Scheme 1. If we knew the stability of Conformer 2 for the **2**·**5** complex (ΔG_2), the double-mutant cycle equation could be applied as follows:

$$\begin{aligned} \text{Aromatic interaction in Complex A} &= \Delta\Delta G \\ &= \Delta G(\mathbf{1} \cdot \mathbf{4}) - \Delta G(\mathbf{2} \cdot \mathbf{4}) - \Delta G(\mathbf{1} \cdot \mathbf{5}) + \Delta G_2 \end{aligned} \quad (8)$$

However, the experimentally determined free energy of complexation of the **2**·**5** complex reflects the population-weighted average of Conformers 1 and 2 (χ_1 and χ_2).

$$\Delta G(\mathbf{2} \cdot \mathbf{5}) = \chi_1 \Delta G_1 + \chi_2 \Delta G_2 \quad (9)$$

But

$$\Delta G_2 - \Delta G_1 = \Delta\Delta G = \text{Aromatic interaction in Complex A} \quad (10)$$

Therefore

$$\chi_2 / \chi_1 = e^{-\Delta\Delta G / RT} \quad (11)$$

By using

$$\chi_2 + \chi_1 = 1 \quad (12)$$

$$\chi_2 = \frac{e^{-\Delta\Delta G / RT}}{1 + e^{-\Delta\Delta G / RT}} \text{ and } \chi_1 = \frac{1}{1 + e^{-\Delta\Delta G / RT}} \quad (13)$$

Substituting into Equation (9) and rearranging gives

$$\Delta G_2 = \Delta G(\mathbf{2} \cdot \mathbf{5}) + \Delta\Delta G / (1 + e^{-\Delta\Delta G / RT}) \quad (14)$$

Substituting into Equation (8) and rearranging, the double-mutant cycle equation for this system becomes

$$\Delta\Delta G - \frac{\Delta\Delta G}{1 + e^{-\Delta\Delta G / RT}} = \Delta G(\mathbf{1} \cdot \mathbf{4}) - \Delta G(\mathbf{2} \cdot \mathbf{4}) - \Delta G(\mathbf{1} \cdot \mathbf{5}) + \Delta G(\mathbf{2} \cdot \mathbf{5}) \quad (15)$$

There is no analytical solution to this equation for $\Delta\Delta G$, but for a given set of $\Delta\Delta G$ values, it is straightforward to construct a look-up table of $\Delta\Delta G - \Delta\Delta G / (1 + e^{-\Delta\Delta G / RT})$ values. This is the free energy that is obtained from the double-mutant cycle by assuming there is no problem of conformational equilibria. Thus we can experimentally determine the apparent aromatic interaction energy by using:

$$\Delta\Delta G_{\text{expt}} = \Delta G(\mathbf{1} \cdot \mathbf{4}) - \Delta G(\mathbf{2} \cdot \mathbf{4}) - \Delta G(\mathbf{1} \cdot \mathbf{5}) + \Delta G(\mathbf{2} \cdot \mathbf{5}) \quad (16)$$

and then use the look-up table to find the actual value of $\Delta\Delta G$. There is an error in the value of $\Delta\Delta G_{\text{expt}}$ that differs from the actual interaction energy by $\Delta\Delta G / (1 + e^{-\Delta\Delta G / RT})$. Figure 3 shows the variation of this error as a function of

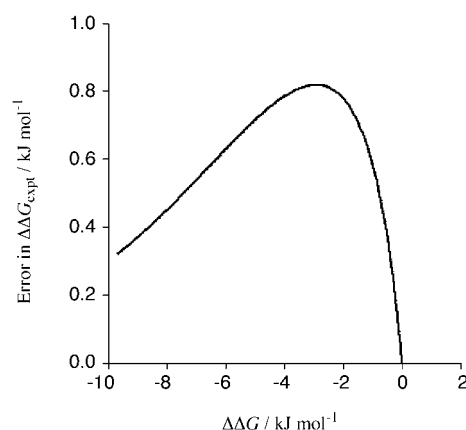
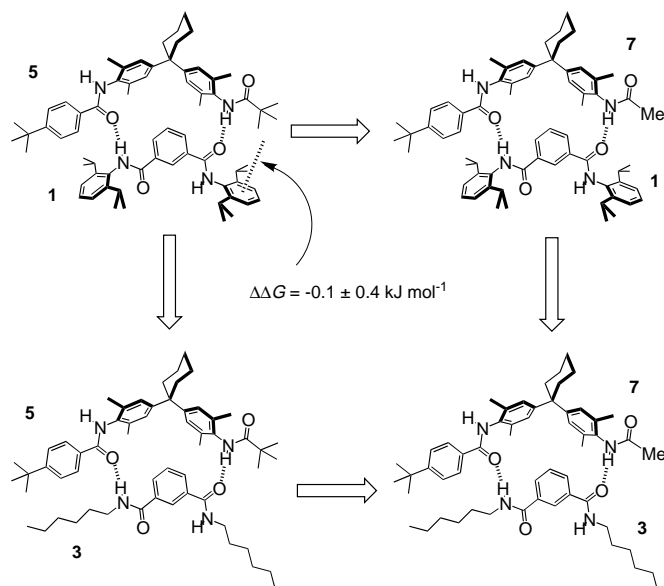


Figure 3. The error in the magnitude of $\Delta\Delta G_{\text{expt}}$ evaluated in the double-mutant cycle shown in Figure 1 and caused by the conformational equilibrium in the **2**·**5** complex shown in Figure 2. $\Delta\Delta G$ is the true value of the edge-to-face aromatic interaction.

$\Delta\Delta G$. When $\Delta\Delta G = 0$, $\Delta G_1 = \Delta G_2$, and so there is no error caused by the presence of a 50:50 mixture of these two degenerate species. As $\Delta\Delta G$ increases, the error increases till it reaches a maximum value of -0.8 kJ mol^{-1} , when $\Delta\Delta G = -3.7 \text{ kJ mol}^{-1}$. As $\Delta\Delta G$ increases further, the error drops again, because Conformer 2 becomes much more stable than Conformer 1, and the small amount of Conformer 1 present represents a minor perturbation to the system. For this system, $\Delta\Delta G_{\text{expt}}$ is $-0.9 \pm 0.4 \text{ kJ mol}^{-1}$, the error is $0.5 \pm 0.2 \text{ kJ mol}^{-1}$, the populations of Conformers 1 and 2 for the **2**·**5** complex are 36% and 64%, respectively, and $\Delta\Delta G$, the edge-to-face aromatic interaction in Complex A, is $-1.4 \pm 0.6 \text{ kJ mol}^{-1}$. This value agrees extremely well with the values obtained from the other three double-mutant cycles discussed above.

Finally, we return to the question of whether the mutated functional groups, the hexyl and *tert*-butyl groups, interact with the adjacent aromatic rings. There is evidence in the literature that *tert*-butyl groups can show significant interactions with the faces of aromatic rings, and clearly this would cause problems with the approach described here.^[3] We therefore prepared the corresponding acetyl compound, **7**, in order to quantify this effect directly. Scheme 8 shows the



Scheme 8. A chemical double-mutant cycle for determining the magnitude of the interaction of a *tert*-butyl group with the face of the aromatic ring in the **1**·**5** complex.

double-mutant cycle used to quantify the *tert*-butyl aromatic interaction in this system. The association constants obtained by using compound **7** are almost identical to those obtained for compound **5**, and the $\Delta\delta$ values are very similar; this indicates that there is no change in the structures of the complexes (Table 1). The double-mutant cycle in Scheme 8 yields a value of $-0.1 \pm 0.4 \text{ kJ mol}^{-1}$ for the *tert*-butyl-aromatic interaction in this system, so the aromatic to *tert*-butyl mutation is appropriate for quantifying aromatic interactions as described above.

Conclusion

We have developed a chemical double-mutant cycle approach to quantifying weak noncovalent interactions. The method works well for edge-to-face aromatic interactions, as described above. By using a series of double-mutant cycles, we have been able to quantify the benzoyl-diisopropyl aniline interaction in chloroform in the zipper Complex **1**·**4** in four different ways, and the results are remarkably consistent: -1.3 ± 0.3 , -1.6 ± 0.4 , -1.4 ± 0.5 and $-1.4 \pm 0.6 \text{ kJ mol}^{-1}$, which yields an average value of $-1.4 \pm 0.5 \text{ kJ mol}^{-1}$. Although there are some limitations of the method, many of the potential errors are removed in the double-mutant cycle. The NMR titrations were carried out under similar conditions for

each compound; this means systematic errors cancel out. For example, the thermodynamic consequences of subtle changes in conformation cancel out if they occur in pairs as discussed for the **3** complexes above. Problems are only encountered when single complexes behave differently from the other three in a cycle, as explained for the **2**·**5** complex that has a different symmetry from the rest. The values of interaction energy determined here are free energies, but implicit in the approach is an assumption that they relate to the enthalpy of interaction and that entropy changes cancel in the cycles. This ignores the consequences of entropy–enthalpy compensation,^[6] but further experiments are required to quantify the magnitude of this effect. Armed with this methodology, we are in a position to tackle quantitative structure–activity relationships for a range of noncovalent interactions.^[8]

Experimental Section

The preparation of **1**, **2a** and **4** have been described previously.^[9] All reagents were purchased from Aldrich and used without further purification.

Compound 2: Compound **2a** (0.50 g, 1.45 mmol) was dissolved in dry dichloromethane (10 mL), and this solution was added dropwise to a stirred solution of *n*-hexylamine (0.20 mL, 0.16 g, 1.6 mmol) and triethylamine (0.11 mL, 0.08 g, 0.79 mmol) over a period of 10 mins. The reaction mixture was stirred for a further 12 h. After workup with HCl (1M, $2 \times 20 \text{ mL}$), NaOH (1M, $2 \times 20 \text{ mL}$) and brine (20 mL), the required product was purified by recrystallisation from dichloromethane and petroleum-ether (40–60) yielding a white powder. Yield: 0.45 g, 75%; m.p. 203–205 °C; ^1H NMR (250 MHz, CDCl_3 , 25 °C, TMS): δ = 8.45 (s, 1H), 8.05 (d, 2H), 7.95 (d, 2H), 7.64 (s, 1H), 7.52 (t, 1H), 7.35 (t, 1H), 7.22 (d, 2H), 6.43 (t, 1H), 3.45 (q, 2H), 3.11 (sept, 2H), 1.60 (quint, 2H), 1.34 (m, 6H), 1.20 (d, 12H), 0.89 (t, 2H); ^{13}C NMR (250 MHz, CDCl_3 , 25 °C, CDCl_3): δ = 166.26, 166.10, 146.60, 135.66, 134.97, 133.10, 130.45, 130.17, 128.96, 128.18, 127.09, 118.29, 31.51, 29.54, 28.65, 26.66, 24.04, 23.77, 22.55, 14.40; FAB[+ve] m/z = 409 $[M+H]^+$, $\text{C}_{26}\text{H}_{36}\text{N}_2\text{O}_2$ requires 408; elemental analysis calcd (%) for $\text{C}_{26}\text{H}_{36}\text{N}_2\text{O}_2$: C 76.43, H 8.88, N 6.86; found C 76.17, H 8.97, N 6.80.

Compound 3: *n*-Hexylamine (1.32 mL, 1.01 g, 0.010 mol) and triethylamine (1.86 mL, 1.34 g, 0.013 mol) were taken up in dry dichloromethane (10 mL) and stirred under argon. Isophthaloyl dichloride (1.02 g, 5.00 mmol) was similarly dissolved in dry dichloromethane (10 mL) and transferred to a dropping funnel. The acid chloride was added to the stirred amine solution over a period of 5 min, and the mixture stirred for 12 h. After workup with HCl (1M, $2 \times 20 \text{ mL}$), NaOH (1M, $2 \times 20 \text{ mL}$) and brine (20 mL), the required product was purified by recrystallisation from dichloromethane and petroleum-ether (40–60) yielding a white powder. Yield: 1.45 g, 87%; m.p. 164–165 °C; ^1H NMR (250 MHz, CDCl_3 , 25 °C, TMS): δ = 8.15 (s, 1H), 7.90 (d, J = 7.2 Hz), 7.50 (t, 1H), 6.25 (t, 2H), 3.45 (q, 4H), 1.61 (quint, 4H), 1.32 (m, 2H), 0.90 (t, 6H); ^{13}C NMR (250 MHz, CDCl_3 , 25 °C, CDCl_3): δ = 166.88, 134.89, 129.92, 128.75, 125.16, 40.28, 31.48, 29.51, 26.67, 22.53, 14.03; FAB[+ve] m/z = 333 $[M+H]^+$, $\text{C}_{32}\text{H}_{42}\text{N}_2\text{O}_2$ requires 332; elemental analysis calcd (%) for $\text{C}_{32}\text{H}_{42}\text{N}_2\text{O}_2$: C 72.25, H 9.70, N 8.43; found C 72.15, H 9.63, N 8.19.

Compound 5a: Bis(aniline) **3** (6.76 g, 0.021 mol) and triethylamine (0.30 mL, 0.21 g, 0.21 mmol) were taken up in dry dichloromethane (40 mL) and stirred at room temperature under argon. 4-*tert*-Butylbenzoyl chloride (0.39 mL, 0.41 g, 0.21 mmol) was similarly dissolved in dry dichloromethane (80 mL), transferred to a dropping funnel and added dropwise to the amine solution over a period of 3 h. After being stirred for 12 h, the reaction mixture was extracted with HCl (5M, $2 \times 100 \text{ mL}$). The aqueous fractions were combined, neutralised by the addition of NaOH pellets and extracted with dichloromethane ($2 \times 100 \text{ mL}$). After drying over anhydrous MgSO_4 the solvent was removed by evaporation under reduced pressure. The fine white powder isolated after crystallisation from dichloromethane with petroleum ether (40–60) was shown to be the required product. Yield: 0.81 g, 80%; m.p. 257–259 °C; ^1H NMR

(250 MHz, CDCl_3 , 25 °C, TMS): δ = 7.84 (d, 2H), 7.52 (d, 2H), 7.26 (s, 1H), 7.01 (s, 2H), 6.86 (s, 2H), 2.22 (s, 6H), 2.16 (s, 6H), 2.22–2.16 (brm, 4H), 1.60–1.40 (brm, 6H), 1.36 (s, 9H); ^{13}C NMR (250 MHz, CDCl_3 , 25 °C, CDCl_3): δ = 176.75, 165.83, 152.54, 147.10, 135.07, 134.89, 131.94, 131.44, 128.84, 126.93, 126.85, 121.23, 111.07, 45.35, 39.17, 37.13, 27.77, 26.41, 22.93, 18.91, 18.66; FAB[+ve] m/z = 483 $[M+H]^+$, $\text{C}_{33}\text{H}_{42}\text{N}_2\text{O}$ requires 482; elemental analysis calcd (%) for $\text{C}_{33}\text{H}_{42}\text{N}_2\text{O}$: C 82.11, H 8.77, N 5.80; found C 81.70, H 8.68, N 6.02.

Compound 5: Trimethylacetyl chloride (0.091 mL, 0.089 g, 0.74 mmol) in dry dichloromethane (2 mL) was added over 10 mins to a stirred suspension of compound **5a** (0.30 g, 0.62 mmol) and triethylamine (0.10 mL, 0.075 g, 0.74 mmol) in dry dichloromethane (5 mL). After 15 min, the suspension had dissolved and the reaction mixture was stirred for a further 10 mins before workup with HCl (1M, 2×10 mL), NaOH (1M, 2×10 mL) and brine (10 mL). The white solid resulting after evaporation of the solvent under reduced pressure was purified by medium-pressure chromatography with dichloromethane eluant. Compound **5** was isolated as a white solid after recrystallisation from dichloromethane and petroleum ether (40–60). Yield: 0.24 g, 68%; m.p. 186–187 °C; ^1H NMR (250 MHz, CDCl_3 , 25 °C, TMS): δ = 7.83 (d, 2H), 7.50 (d, 2H), 7.40 (s, 1H), 7.00 (s, 2H), 6.98 (s, 2H), 6.90 (s, 1H), 2.28–2.19 (brm, 4H), 2.20 (s, 6H), 2.15 (s, 6H), 1.60–1.40 (brm, 6H), 1.37 (s, 9H), 1.30 (s, 9H); ^{13}C NMR (250 MHz, CDCl_3 , 25 °C, CDCl_3): δ = 176.58, 165.76, 155.21, 147.50, 146.97, 134.93, 134.83, 131.77, 131.34, 127.09, 126.99, 125.64, 53.45, 45.39, 39.23, 37.09, 31.18, 27.80, 26.34, 22.88, 18.88, 18.67; FAB[+ve] m/z = 567 $[M+H]^+$, $\text{C}_{38}\text{H}_{50}\text{N}_2\text{O}_2$ requires 566; elemental analysis calcd (%) for $\text{C}_{38}\text{H}_{50}\text{N}_2\text{O}_2 \cdot 0.5\text{H}_2\text{O}$: C 79.26, H 8.93, N 4.86; found C 79.51, H 8.79, N 4.80.

Compound 6: Trimethylacetyl chloride (1.15 mL, 1.12 g, 9.3 mmol) was added to a stirred solution of bisaniline (1.00 g, 3.1 mmol) and triethylamine (0.45 mL, 0.34 g, 3.1 mmol) in dry dichloromethane (20 mL). The reaction mixture was stirred for 12 h before workup with HCl (1M, 2×20 mL), NaOH (1M, 2×20 mL) and brine (20 mL). After drying over anhydrous MgSO_4 , the solvent was removed under reduced pressure. The product was passed through a silica plug with dichloromethane eluant prior to recrystallisation from dichloromethane and petroleum ether (40–60) which yielded a white powder. Yield: 1.26 g, 83%; m.p. 265–267 °C; ^1H NMR (250 MHz, CDCl_3 , 25 °C, TMS): δ = 6.90 (s, 4H), 6.74 (s, 2H), 2.17 (brm, 4H), 2.12 (s, 12H), 1.45–1.60 (brm, 6H), 1.32 (s, 18H); ^{13}C NMR (250 MHz, CDCl_3 , 25 °C, CDCl_3): δ = 176.6, 147.0, 134.8, 126.9, 45.4, 39.1, 37.2, 27.7, 26.4, 22.9, 18.6; FAB[+ve] m/z = 490 $[M+H]^+$, $\text{C}_{32}\text{H}_{46}\text{N}_2\text{O}_2$ requires 489; elemental analysis calcd (%) for $\text{C}_{32}\text{H}_{46}\text{N}_2\text{O}_2$: C 78.32, H 9.45, N 5.71; found C 78.30, H 9.72, N 5.50.

Compound 7: Compound **5a** (0.37 g, 0.77 mmol) and glacial acetic acid (0.043 mL, 0.046 g, 0.77 mmol) were suspended in dry dichloromethane (10 mL) and cooled to 0 °C in an ice bath. After the mixture had been stirred for 15 mins, 1.3 equivalents of EDC were added, and the reaction mixture was stirred for 12 h. The mixture was washed with HCl (1M, 2×20 mL), NaOH (1M, 2×20 mL) and brine (20 mL), and the solvent was removed under reduced pressure to yield a brown oil, which was purified by medium pressure chromatography with dichloromethane eluant. The required product **7** was isolated as a white powder after recrystallisation from dichloromethane and petroleum ether (40–60). Yield: 0.21 g, 53%; m.p. 164–166 °C; ^1H NMR (250 MHz, $[\text{D}_6]\text{DMSO}$, 25 °C, TMS): δ = 9.55 (s, 1H), 9.09 (s, 1H), 7.90 (d, 2H), 7.54 (d, 2H), 7.07 (s, 2H), 7.00 (s, 2H), 2.32–2.20 (brm, 4H), 2.20 (s, 6H), 2.10 (s, 6H), 2.00 (s, 3H), 1.60–1.40 (brm, 6H), 1.32 (s, 9H); ^{13}C NMR (250 MHz, $[\text{D}_6]\text{DMSO}$, 25 °C, CDCl_3): δ = 168.31, 165.27, 154.72, 146.83, 135.60, 134.98, 133.17, 132.12, 127.76, 126.55, 126.30, 125.68, 45.13, 36.61, 35.12, 31.42, 26.26, 23.03, 19.01, 18.94; FAB[+ve] m/z = 525 $[M+H]^+$, $\text{C}_{35}\text{H}_{44}\text{N}_2\text{O}_2$ requires 524.

NMR binding experiments: ^1H NMR dilution experiments were used to check whether dimerisation of compounds **1–7** was significant at the concentrations used. All dimerisation constants are less than 1M^{-1} and so do not affect the titrations to any extent. A 3.0 mL sample of host of known concentration (2–5 mM) was prepared in CDCl_3 , 0.8 mL of this solution was removed, and a ^1H NMR spectrum was recorded. An accurately weighed sample of the guest was then dissolved in the remaining 2.2 mL of host solution. This solution was almost saturated with guest (100–200 mM), to allow access to as much of the binding isotherm as possible (50–80% saturation was achieved), and contained host so that the host concentration remained constant during the titration. Aliquots of guest solution were added successively to the NMR tube containing the host solution, the tube

was shaken to mix the host and guest solutions, and the ^1H NMR spectra were recorded after each addition. For signals that moved more than 0.01 ppm, the chemical shifts at all concentrations of guest were recorded and analysed by using purpose-written software, *NMRTit HG*, on an Apple Macintosh microcomputer.^[10] This programme fits the data to a 1:1 binding model to yield the association constant, the bound chemical shifts in the HG complex and, if required, the free chemical shifts of the unbound species. All titrations were repeated at least three times and, where possible, the identities of the host and guest were reversed in order to obtain accurate $\Delta\delta$ values for both binding partners. Where this was not possible, the binding constant determined by fitting the host signals was fixed, and *NMRTit HG* was used to analyse the changes in the guest signals to extract the bound-guest chemical shift. The mean association constant for each experiment was evaluated as the weighted mean (based on the observed change in chemical shift) of the association constants for the individual signals monitored. The error was taken as twice the standard error. The values of K_a quoted in Table 1 are the average values and errors from at least three separate experiments. Two-dimensional ROESY spectra were recorded on a Bruker AMX-2-400 by using a 300 ms mixing time and a 3 s delay between pulses.

NMR Structure Determination: The method used to determine three-dimensional structures from complexation-induced changes in chemical shift and its application to determining the structure of Complex **1–4** has been described in detail elsewhere.^[5] The conformational search for Complex **3–4** was carried out by using the same procedure. The hexyl chains of **3** were replaced by methyl groups, and the structure was minimised by using the MM3 force-field in MacroModel.^[11] Compound **4** was also constructed in MacroModel and energy minimised by using the MM3 force-field. A genetic algorithm was used to optimise the conformation of the complex so that the calculated $\Delta\delta$ values matched the experimental values as closely as possible (Table 1). We allowed intermolecular translation (± 10 Å) and rotation ($\pm 180^\circ$) as well as intramolecular torsional changes ($\pm 180^\circ$) for all single bonds in both molecules (excluding the amide C–N bonds and the cyclohexyl group). The experimentally observed intermolecular NOEs between **j** and **a** and **b** were used to restrict the search space. Van der Waals clashes were penalised at distances of less than 3 Å for intermolecular clashes and 2 Å for intramolecular clashes for nonhydrogen atoms. The search converged to values of $R_{\text{expt}}/R_{\Delta\delta}$ of 9.0 in about 2000 generations for a population of 200 (R_{expt} is the root mean square $\Delta\delta$ of the experimentally observed $\Delta\delta$ values, and $R_{\Delta\delta}$ is the RMS difference between the calculated and experimental values).

Acknowledgement

We thank the EPSRC (F.J.C.), the University of Sheffield (J.F.M.), Merck Sharp and Dohme (F.J.C.), SmithKline Beecham (J.F.M.), the European Union (P.T.) and the Lister Institute (C.A.H.) for financial support. We thank Dr. C. J. Craven and Dr. J. P. Waltho for 600 MHz NMR spectra. We also thank the Royal Society/NATO & FCO Chevening (M.O.V.), the Lister Institute (C.A.H.), the EPSRC (M.J.P.) and the James Black Foundation (C.Z.) for funding.

- [1] a) D. H. Williams, M. S. Westwell, *Chem. Soc. Rev.* **1998**, 27, 57–63; b) D. H. Williams, M. S. Searle, J. P. Mackay, U. Gerhard, R. A. Maplestone, *Proc. Natl. Acad. Sci. USA* **1993**, 90, 1172–1178.
- [2] a) L. Serrano, M. Bycroft, A. R. Fersht, *J. Mol. Biol.* **1991**, 218, 465–475; b) A. Horovitz, A. R. Fersht, *J. Mol. Biol.* **1990**, 214, 613–617; c) A. R. Fersht, G. Schreiber, *J. Mol. Biol.* **1995**, 248, 478–486; d) D. P. O'Brien, R. M. H. Entress, M. A. Cooper, S. W. O'Brien, A. Hopkinson, D. H. Williams, *J. Am. Chem. Soc.* **1999**, 121, 5259–5265; e) D. H. Williams, A. J. Maguire, W. Tsuzuki, M. S. Westwell, *Science* **1998**, 280, 711–714; f) D. H. Williams, M. S. Westwell, *Chem. Biol.* **1996**, 3, 695–701.
- [3] a) S. B. Ferguson, F. Diederich, *Angew. Chem.* **1986**, 98, 1127–1129; *Angew. Chem. Int. Ed. Engl.* **1986**, 25, 1127–1129; b) A. D. Hamilton, D. Van Engen, *J. Am. Chem. Soc.* **1987**, 109, 5035–5036; c) J. Rebek, B. Askew, P. Ballester, C. Buhr, S. Jones, D. Nemeth, K. Williams, *J. Am. Chem. Soc.* **1987**, 109, 5033–5035; d) T. J. Sheppard, M. A. Petti, D. A. Dougherty, *J. Am. Chem. Soc.* **1988**, 110, 1983–1985; e) S. C.

- Zimmerman, C. M. Vanzyl, G. S. Hamilton, *J. Am. Chem. Soc.* **1989**, *111*, 1373–1381; f) D. B. Smithrud, F. Diederich, *J. Am. Chem. Soc.* **1990**, *112*, 339–343; g) C. A. Hunter, M. N. Meah, J. K. M. Sanders, *J. Am. Chem. Soc.* **1990**, *112*, 5773–5780; h) P. L. Anelli, N. Spencer, J. F. Stoddart, *J. Am. Chem. Soc.* **1991**, *113*, 5131–5133; i) F. Cozzi, M. Cinquini, R. Annunziata, T. Dwyer, J. S. Siegel, *J. Am. Chem. Soc.* **1992**, *114*, 5729–5733; j) M. Crego, C. Raposo, C. M. Caballero, E. Garcia, J. G. Saez, J. R. Moran, *Tetrahedron Lett.* **1992**, *33*, 7437–7440; k) A. W. Schwabacher, S. Zhang, W. Davy, *J. Am. Chem. Soc.* **1993**, *115*, 6995–6996; l) S. Paliwal, S. Geib, C. S. Wilcox, *J. Am. Chem. Soc.* **1994**, *116*, 4497–4498; m) R. S. Lokey, B. L. Iverson, *Nature* **1995**, *375*, 303–305; n) L. F. Newcomb, T. S. Haque, S. H. Gellman, *J. Am. Chem. Soc.* **1995**, *117*, 6509–6519; o) D. B. Amabilino, P. R. Ashton, C. L. Brown, E. Cordova, L. A. Godinez, T. T. Goodnow, A. E. Kaifer, S. P. Newton, M. Pietraszkiewicz, D. Philp, F. M. Raymo, A. S. Reder, M. T. Rutland, A. M. Z. Slawin, N. Spencer, J. F. Stoddart, D. J. Williams, *J. Am. Chem. Soc.* **1995**, *117*, 1271–1293; p) A. S. Shetty, J. S. Zhang, J. S. Moore, *J. Am. Chem. Soc.* **1996**, *118*, 1019–1027; q) J. N. H. Reek, A. H. Priem, H. Engelkamp, A. E. Rowan, J. Elemans, R. J. M. Nolte, *J. Am. Chem. Soc.* **1997**, *119*, 9956–9964; r) N. J. Heaton, P. Bello, B. Herrandon, A. del Campo, J. Jimenez-Barbero, *J. Am. Chem. Soc.* **1998**, *120*, 12371–12384; s) G. A. Breault, C. A. Hunter, P. C. Mayers, *J. Am. Chem. Soc.* **1998**, *120*, 3402–3410.
- [4] a) H. Adams, F. J. Carver, C. A. Hunter, J. C. Morales, E. M. Seward, *Angew. Chem.* **1996**, *108*, 1628–1631; *Angew. Chem. Int. Ed. Engl.* **1996**, *35*, 1542–1544; b) H. Adams, K. D. M. Harris, G. A. Hembury, C. A. Hunter, D. J. Livingstone, J. F. McCabe, *Chem. Commun.* **1996**, 2531–2532; c) F. J. Carver, C. A. Hunter, E. M. Seward, *Chem. Commun.* **1998**, 775–776.
- [5] M. J. Packer, C. A. Hunter, *Chem. Eur. J.* **1999**, *5*, 1891–1897.
- [6] a) M. S. Searle, G. J. Sharman, P. Groves, B. Benhamu, D. A. Beauregard, M. S. Westwell, R. J. Dancer, A. J. Maguire, A. C. Try, D. H. Williams, *J. Chem. Soc. Perkin Trans. 1* **1996**, *23*, 2781–2786; b) M. S. Searle, D. H. Williams, *J. Am. Chem. Soc.* **1992**, *114*, 4497–4498, 10690–10697.
- [7] M. Herail, E. Megnassan, A. Proutière, *J. Phys. Org. Chem.* **1997**, *10*, 167–174.
- [8] F. J. Carver, G. Chessari, C. A. Hunter, D. J. Livingstone, C. M. R. Low, J. F. McCabe, M. J. Packer, E. M. Seward, J. G. Vinter, C. Zonta, unpublished results.
- [9] a) C. A. Hunter, *J. Am. Chem. Soc.* **1992**, *114*, 5303–5311; b) A. P. Bisson, F. J. Carver, D. S. Eggleston, R. C. Haltiwanger, C. A. Hunter, D. L. Livingstone, J. F. McCabe, C. Rotger, A. E. Rowan, *J. Am. Chem. Soc.* **2000**, *122*, 8856–8868.
- [10] A. P. Bisson, C. A. Hunter, J. C. Morales, K. Young, *Chem. Eur. J.* **1998**, *4*, 845–851.
- [11] F. Mohamadi, N. G. J. Richards, W. C. Guida, R. Liskamp, M. Lipton, C. Caufield, G. Chang, T. Hendrickson, W. C. Still, *J. Comp. Chem.* **1990**, *11*, 440–467.

Received: May 8, 2001 [F3245]